Saharan Aerosols over the South of France: Characterization Derived from Satellite Data and Ground Based Measurements

J. L. DEUZE, C. DEVAUX, M. HERMAN, R. SANTER AND D. TANRE

Laboratoire d'Optique Atmosphérique, Université des Sciences et Techniques de Lille, France

20 May 1987 and 28 September 1987

ABSTRACT

In July 1983, the summer transport of Saharian aerosols across the Mediterranean Sea was observed. The dust cloud was particularly dense and was clearly detected in A.V.H.R.R. and METEOSAT imageries. Optical thicknesses and Angström coefficients have been derived from these pictures. During the same period, ground based observations—transmission, aureole and polarization measurements—were performed at the Observatoire de Haute Provence (southeast of France). Measured aerosol optical thicknesses at 550 nm were as large as about 1.5.

The optical thicknesses and Angström coefficients derived from the two experiments are compared and are in good agreement.

1. Introduction

In summertime, westward migrations of saharan dust clouds over the tropical North Atlantic Ocean are commonly observed from satellite imagery. Local and time variations of the dust have been described by Carlson and Prospero (1972). The aerosol optical thickness has been derived from satellite data in the visible range (Carlson et al. 1977; Norton et al. 1980; Griggs 1979; Koepke and Quenzel 1979). The integrated mass of dust was obtained by Fraser (1976). Dust outbreaks have also been observed over the eastern Mediterranean Sea by Mekler et al. (1977) and Otterman et al. (1982). These dust clouds have also appeared during nightime in the METEOSAT IR channel (Legrand et al. 1985).

During July 1983, ground based measurements were planed at the O.H.P. ("Observatoire de Haute Provence", about 80 km from the mediterranean coast with an altitude of 1900 m) in order to observe the El Chichon stratospheric layer. This objective was disturbed by the occurrence of a saharan dust outbreak, which provided the opportunity to characterize this dust cloud from ground measurements.

This event was looked for in the AVHRR (on NOAA-7) and METEOSAT imageries over the Mediterranean Sea. Thus, we have the interesting possibility of comparing aerosol characterization derived from satellite imagery with a more detailed characterization derived from ground observations. We will show that the aerosol thickness (τ_a) and the Angström coefficient deduced from satellite data are in good agreement with the ground measurements.

2. The ground based measurements

a. *Presentation of the measurements, from 26 July to 29 July 1983*

Extinction measurements were performed with two multispectral radiometers. The first one has a silicium detector and covers the range from 440 to 1100 nm; the second has a PbS detector, and performs measurements up to 3000 nm. The two radiometers had been previously calibrated, (April 1983), using Langley plots. The seven band measurements are centered at 445, 551, 648, 864, 1040, 1586 and 2208 nm.

In the wavelength range of our band measurements, water vapor and ozone absorption is simply a corrective term. This gaseous absorption was merely computed from LOWTRAN-5 code (Kneizys et al. 1980), by using the climatologic value of London et al. (1976) for the ozone content, and the midlatitude summer model of Mc Clatchey et al. (1970) for the water vapor content. The Rayleigh optical thickness was estimated from the pressure measurements. By subtracting Rayleigh scattering and gaseous absorption components from the total optical thickness, we obtained the aerosol optical thickness τ_a. Figure 1 gives τ_a versus the UTC time, at $\lambda = 550$ nm, for the 4 observation days. On the morning of 26 July, the aerosol content was almost constant and Langley plots drawn from these data confirmed the previous calibration. Despite the high altitude of the site (1900 m), τ_a was always very large, with a maximum of 1.7 on 27 July, which is quite an un-

Corresponding author address: Dr. J. L. Deuze, Laboratoire D'Optique Atmospherique, Universite Des Sciences Et Techniques De Lille, 59655 Villeneuve D'Ascq Cedex, France.

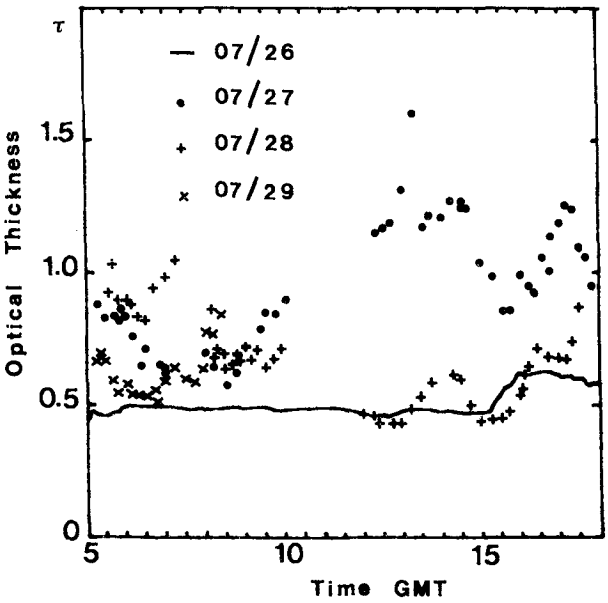

FIG. 1. Instantaneous aerosol optical thickness τ_a, at 550 nm, for the 4 days. A full line has been drawn through the smooth measurements obtained on 26 July. The symbols for other days are included on the figure. It was initially planned that the traditional Langley technique would be used to derive τ_a, so that no extinction measurements were performed around noon, when the air mass did not vary; this explains the lack of information, from 1000 to 1300 UTC, in Fig. 1.

usual value. Note that it is unlikely that cirrus clouds could explain these large values of τ_a. The sky was routinely observed around the sun disk, using cross-polaroids in order to attenuate the sun irradiance, and no cirrus clouds were observed during the campaign.

The spectral dependence of the aerosol optical thickness, $\tau_a(\lambda)$, proved to be nearly constant for a given day, but exhibited large variations from day to day. Figure 2 shows the $\tau_a(\lambda)$ behavior observed for the 4 days. On 27 July, the aerosol optical thickness increased largely in the blue range. For the other days, the spectral variation was more flat, mainly on 29 July where the optical thickness was almost constant in the visible range, and decreased slowly at near-IR wavelengths. Figure 2 shows that, through the large investigated spectral range, the $\tau_a(\lambda)$ behavior could not be accounted for with a single Angström coefficient. Therefore, the log–log plots of $\tau_a(\lambda)$ versus λ, in Fig. 2, were crudely fitted by two linear laws, from 445 to 668 nm and from 668 to 1650 nm, thus providing two Angström coefficients, hereafter noted α_v and α_{IR}, respectively. In Table 1, we reported for the 4 days the values obtained for α_v and α_{IR}. The large value of α_v proves the presence of small particles on 27 July, whereas larger particles were predominant on 29 July. The mean deviations $\Delta\alpha_v$ (or $\Delta\alpha_{IR}$) (see Table 1) showed fairly good stability of the aerosol size distribution for a given day, as noted previously. Deviations of the Angström coefficients were somewhat larger in near-IR than in the visible, as a result of the larger measurement errors.

Aureole measurements were performed at $\lambda = 850$ nm, using a silicium detector with an aperture angle of 1°. About 5 min were needed to scan scattering angles from 2° to 30°; the observations were performed

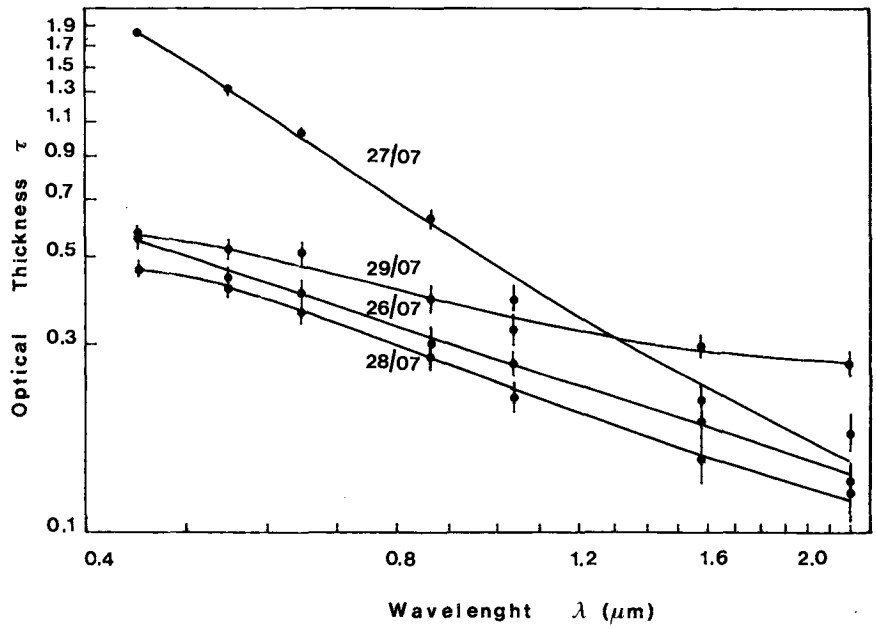

FIG. 2. Aerosol optical thickness as a function of the wavelength for the 4 days. The circles correspond to the measurements, and bars indicate the estimated errors. The solid lines represent the optical thickness spectral dependence computed with the retrieved size distribution.

TABLE 1. Summary of the ground-based measurements (see text): P_{max}, maximum value of the polarization ratio, and $p(\theta)$, particle phase function.

Variable	26 July	27 July	28 July	29 July
α_v	0.70	1.42	0.46	0.18
α_{IR}	1.24	2.06	0.91	0.63
$\Delta\alpha_v$	0.01	0.02	0.02	0.01
$\Delta\alpha_{IR}$	0.07	0.08	0.06	0.08
P_{max} 850 nm	22	51	/	18
P_{max} 1650 nm	16	41	/	18
$\rho(2°)/\rho(10°)$	4.39	/	6.32	7.91

in the amulcantar region, and corrections for multiple scattering were applied, according to Weinman et al. (1975), using the optical thickness measured during the scan.

Unfortunately, the aureolemetre rotation speed was subject to large uncertainties due to high wind speeds during the observations. Although the measurements are only indicative, the increase of the forward scattering from 26 to 29 July (see Table 1) is well correlated with the Angström coefficient variation, and confirms the presence of larger particles on 29 July.

Finally, polarization measurements were performed at near-infrared wavelengths (850 and 1650 nm). The polarimeter scanned the sun incident plane, at low solar elevations to reach backscattering directions. The polarization ratios are reported in Fig. 3, versus the scattering angle. On 27 July, a large contamination by small particles was made evident by the large polarization ratios, whereas both the measurements on 26 and 29 July corresponded to larger particles. Thus, polarization measurements were consistent with the extinction and aureole measurements.

b. Interpretation of the measurements

The aerosol size distribution was retrieved from the optical thicknesses measured in the seven channels, from 445 to 2208 nm, by using the constrained linear inversion scheme developed by King et al. (1978). Six classes of abundance were derived, within the range 0.1–4 μm for 26 and 27 July, and within the range 0.15–6 μm for the 2 last days, to take into account the increase of the large particles. According to the estimate of Patterson et al. (1977), the real part of the refractive index of desert aerosols lies in about 1.55. Desert aerosols are absorbing (WMO 1986), but the imaginary part of their refractive index is probably no more than

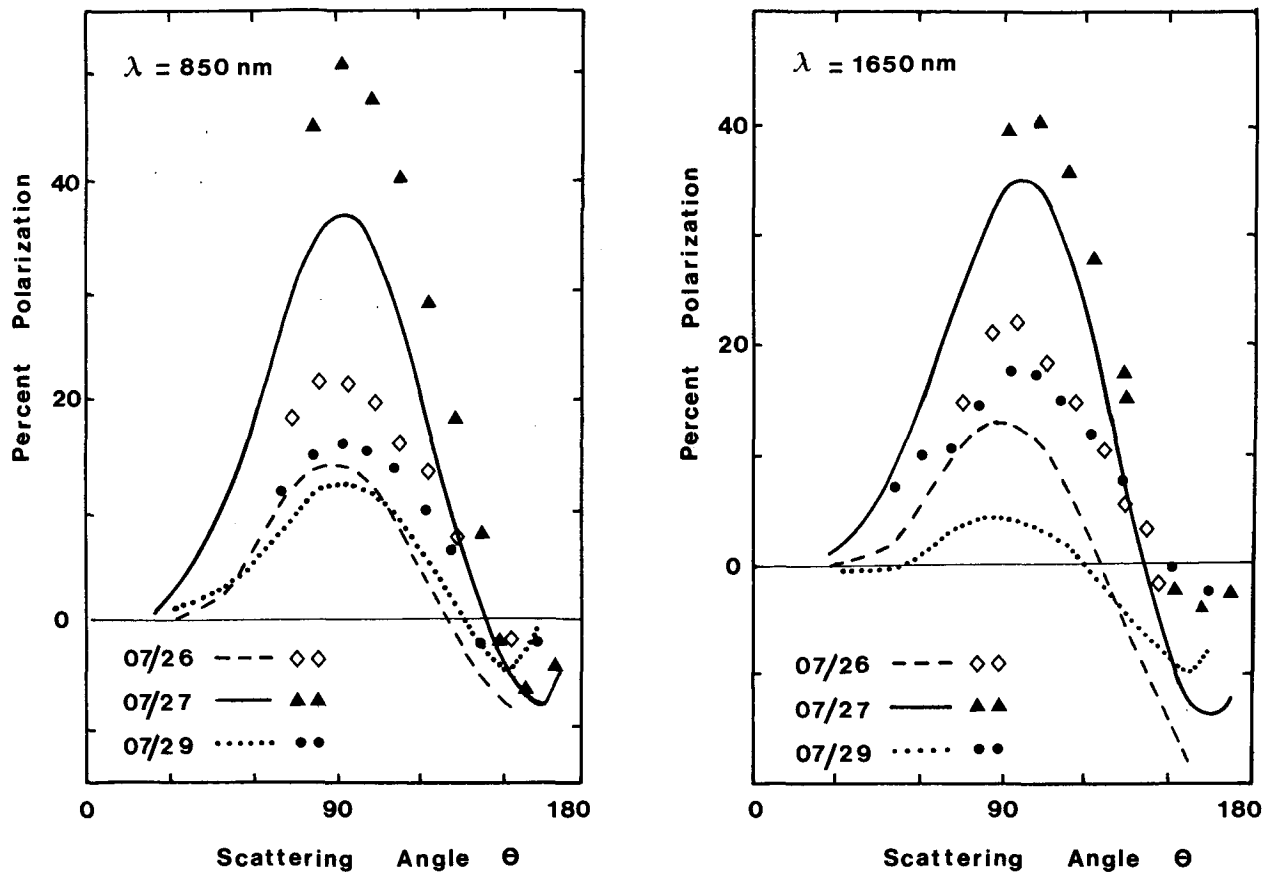

FIG. 3. Percent of polarization as a function of the scattering angle at two wavelengths (850 and 1650 nm) for 3 days (26, 27 and 29 July). The symbols correspond to the measurements, the solid lines to the theoretical computations.

0.005 (Fouquart et al. 1986). Mie calculations prove that so slight an absorption has negligible effect on the spectral dependence of $\tau_a(\lambda)$ and on the polarization ratio for single scattering (Santer 1984), and the inversion was run for an assumed real refractive index, $m = 1.55$.

The results are reported in Fig. 4. The vertical scale applies to the results for 29 July (uppermost curve), and the curves for the other days have been successively displaced downward by a factor of 10 to avoid confusing superposition of the plots. From 26 to 27 July, the particle abundance in the first class increased by one order of magnitude. The large optical thicknesses observed on 27 July thus corresponded to a large addition of small particles of about 0.1 μm radius. The size distributions were quite similar on 26 and 28 July. On 29 July, Fig. 4 shows the occurrence of a bimodal structure of the aerosol size distribution.

As noted previously, the poor quality of the aureole measurements prevents quantitative analysis of these data. On the other hand, the polarimeter was operated for the first time on this occasion and the polarization data deserve some caution. Nevertheless, they have been compared tentatively with the transmission measurements as follows.

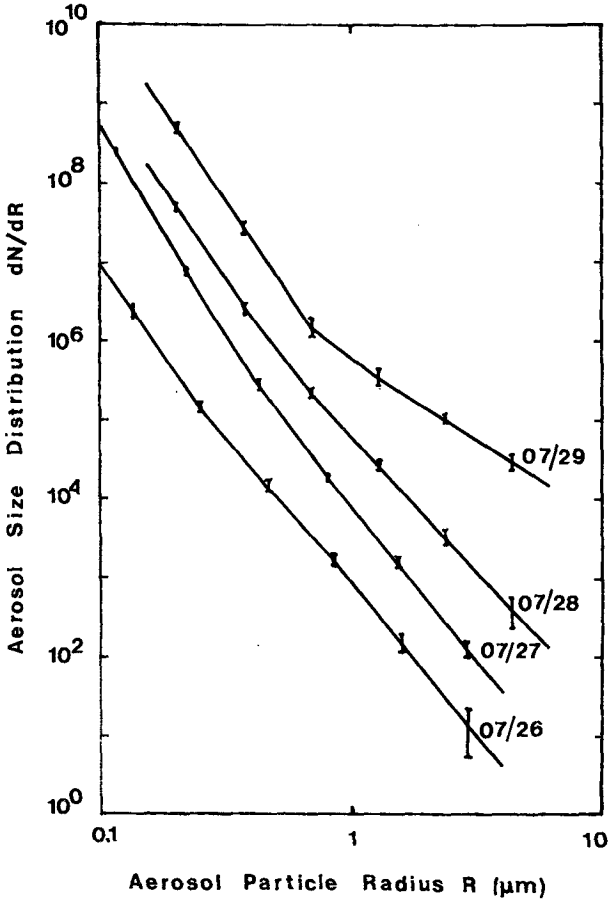

FIG. 4. Aerosol size distributions inverted from the aerosol spectral optical thickness, $\tau_a(\lambda)$. The date is labeled for each curve. The vertical scale applies to the results of 29 July (uppermost curve), and the curves corresponding to the other days have been successively translated downward by a factor of 10. The error bars correspond to the errors on $n(r)$ resulting, in the inversion method, from the experimental errors on $\tau_a(\lambda)$ (error bars in Fig. 2).

Radiative transfer calculations for polarized light were performed for atmosphere models including the appropriate Rayleigh scattering and ground reflectance, and the aerosol component derived from the transmission measurement. The ground-based station was set up in a mountain site with a patchy landscape of bare soils, rocks and meadows, whose mean reflectance was estimated to be about 0.2. As a matter of fact, polarization measurements were performed with low solar elevations, and, thus, with low ground illuminations, so that large inaccuracy in the ground reflectance would have very small influence on the calculated polarization of the sky light. For the aerosol component, the size distribution was fixed according to Fig. 4, the optical thickness was fixed according to the $\tau_a(\lambda)$ measurements performed during the polarimeter scanning and we considered conservative particles. The computed polarization ratios have been reported in Fig. 3 to be compared with the measurements.

The agreement is not at all perfect, and large discrepancies appear, both near the polarization maxima and in backward scattering directions. In fact, by slightly modifying either the particle refractive index or the particle size distribution (particularly, by extrapolating differently $n(r)$ outside the radius range, 0.1 μm–4 μm, in Fig. 4), the observations may be matched more closely in Fig. 3. Such improvements, however, are questionable and raise difficult problems which are beyond the scope of this paper. On the other hand, despite their defects, the predicted polarization ratios are very consistent with the main observed features, especially concerning the time variations and the small particle event on 27 July, and this semiquantitative agreement is encouraging.

Although the aureole and polarization measurements performed during the experiment were very preliminary and were only partly successful, they look promising. Such observations may certainly complement transmission measurement for aerosol characterization. Concerning the main objective of this paper, i.e., the ground validation of satellite observations, the consistency of the whole set of measurements gives an improved confidence in the optical thickness determination.

There may be different explanations, including differences in the source region, for the observed variations of the aerosol characteristics. But, even for a given source area (probably around Chad lake, at this period), the aerosol size distribution may change in connection with the importance of the dust storm. During the ECLATS field experiment, Fouquart et al. (1987) pointed out a clear correlation between the aerosol abundance and their size distribution, with an unexpected amount of small particles for the most turbid

days. We note that this is in accordance with the present observations corresponding to the 27 July event.

3. Satellite data

Desert aerosols are known to be a climatic parameter and it seems valuable to obtain their spatial and time variations at climatic scales in order to include these data in general circulation models. It seems interesting to derive these informations from B2 METEOSAT products, which have been set up to support the International Satellite Cloud Climatology Project (ISCCP). The B2 data are sampled at 3-h intervals and the spatial resolution is 30 km × 30 km. We are developing an algorithm in order to detect dust storms over oceans and estimate their optical thickness from such imagery. This algorithm was applied to the METEOSAT data for 27 July over the Mediterranean Sea. Moreover, as AVHRR images were available for 29 July over the same area, we derived the dust Angström coefficient from these AVHRR data. They are in a good agreement with the ground based measurements.

a. METEOSAT imagery

The problem is to deduce a quantitative estimate of the aerosol loading from satellite pictures. That is easy over ocean surfaces for cloudless conditions, since the atmospheric radiance then depends mainly on the aerosol optical thickness.

By chance no clouds appeared in the METEOSAT imagery of 27 July, so that we were able to localize easily the dust cloud in the pictures. As an example Fig. 5 displays the METEOSAT picture of 1130 UTC. The figure corresponds to the full resolution of the B2 data, with every pixel labeled according to its digital count, as indicated. The picture looks very clear; Sardinia, Corsica, Sicilia and the entire coastal areas are clearly recognizable. However, from the coasts towards a maximum located west of Sardinia, the reflectance

FIG. 5. The figure shows the METEOSAT picture of 27 July at 1130 UTC, over the Mediterranean Sea. Every B2 pixel has been displayed, with different label according to its digital count. The W label corresponds to a digital count larger than 60, and no label corresponds to a digital count smaller than 20 (clear sky). The coasts are well recognizable and no cloud structure appear with sharp edges and large reflectances. The reflectance behavior in the middle of the picture indicates the large and smooth saharan dust cloud.

increases weakly but distinctly. The smoothness and the weakness of the reflectance behavior clearly does not correspond to a cloud structure, but to a dust haze. Therefore, any pixel over the sea which had a digital count (CN) equal or greater than 20 (for the 8-bit-count; i.e., two times the radiance corresponding to the molecular scattering and the mean ocean reflectance) was selected and was considered as corresponding to the aerosol cloud.

The above treatment provided localization of the dust cloud. In order to quantify the phenomena, we first converted digital counts to radiance values, by using the calibration coefficients given by Koepke (1982). Then we corrected these radiances from the Rayleigh scattering contribution and from the gaseous atmosphere effect, by assuming the same previous atmosphere model. Finally, the optical thickness τ_a was derived from these corrected radiances L_a. Here, L_a mainly correspond to single scattered radiation and provide with a good accuracy

$$\tau_a = \frac{4\pi\mu_v L_a}{p_a(\theta)E_0} \tag{1}$$

as shown by Deschamps et al. (1983). In Eq. (1), E_0 is the solar irradiance, θ the scattering angle, $\mu_v = \cos\theta_v$ the cosinus of the viewing direction, and $p_a(\theta)$ the aerosol phase function, which was computed from the desert aerosol model defined by the international radiation commission (WMO 1986).

The above procedure was applied to the METEOSAT pictures of 27 July. The spatial distributions of the aerosol optical thickness derived for the three pictures (0830, 1130 and 1430 UTC) have been drawn in Fig. 6. We have drawn optical depths isolines for τ = 0.5, 1.0 and 1.5. Each picture provides a well-defined geographical repartition of the cloud. The cloud evolution from one picture to the next is very coherent, and the time evolution is consistent with the wind speed (20 km h^{-1}) measured at the Meteorological Office of Nimes-Courbessac. The cloud observed at 0830 UTC is retrieved in the two other scenes (1130 and 1430 UTC) at distances consistent with this speed. Moreover, we selected a fixed point, P, over the sea, located about 120 km south from the OHP; P is marked by a cross in the maps of Fig. 5. The time evolution of the optical thicknesses observed, respectively over this point P from METEOSAT and over the OHP from the ground measurements, are compared in Fig. 7. The two measurements are very consistent since the cloud takes 6 hours to reach the OHP, with respect to the overpass pixel hour.

b. AVHRR imagery

A visible spectral study from AVHRR on NOAA-7 has also been completed. The study was used to obtain an idea of the type of particles through the Angström coefficient. The polar orbiting satellite, named "NOAA series", contains the Advanced Very High Resolution Radiometer (AVHRR) which includes two visible and three infrared channels. We considered only the 0.55–0.90 and 0.725–1.10 μm visible channels (Malila and Anderson 1986).

Unfortunately, during the dust event, we only had data for 29 July; the data for 26 and 27 July were not available and those for 28 July were very contaminated by the glitter effect. By the same method as for the METEOSAT study, we derived the aerosol reflectance by correcting data for Rayleigh and gaseous effects.

From these two reflectances, $\rho_a(\lambda_1)$ and $\rho_a(\lambda_2)$, we inferred an Angström coefficient α_a:

$$\alpha_a = -\frac{\log(\rho_a(\lambda_1)/\rho_a(\lambda_2))}{\log(\lambda_1/\lambda_2)}. \tag{2}$$

In Eq. (2), λ_1 and λ_2 are the centroïd wavelengths λ_C defined by

$$\lambda_C = \frac{\int_0^\infty \lambda E_0(\lambda)R(\lambda)d\lambda}{\int_0^\infty E_0(\lambda)R(\lambda)d\lambda} \tag{3}$$

where $R(\lambda)$ is the spectral response of the sensor. Therefore, for NOAA-7, λ_1 = 633 nm and λ_2 = 848 nm.

The order of magnitude of α_a retrieved by this method is α_a = 0.57. This small value confirms the

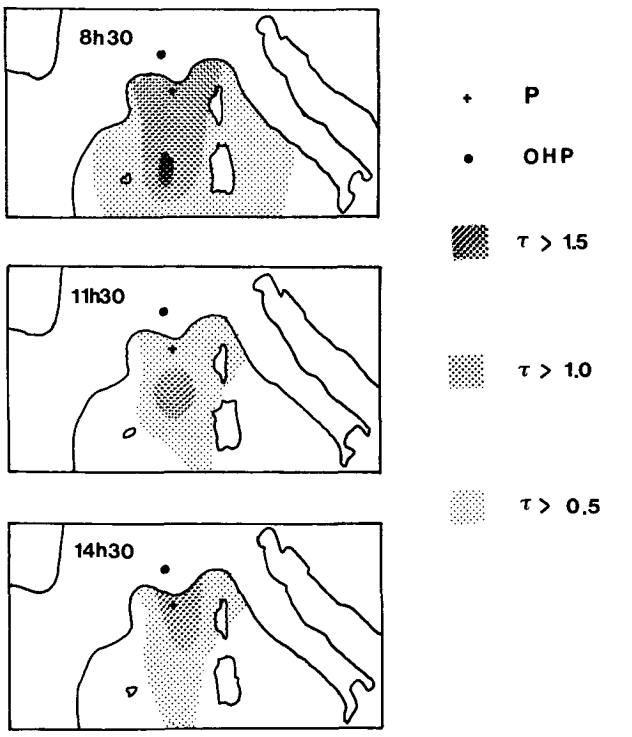

FIG. 6. Maps of the aerosol cloud over the Mediterranean Sea retrieved from METEOSAT data for 0830, 1130 and 1430 UTC. The dust outbreak maximum is observed on the first map, where the area located west of Sardinia presents optical thicknesses larger than 1.5. The importance of the dust outbreak decreases slightly all along the day, but the main features of the optical thickness isolines are similar from map to map, with a motion towards the North.

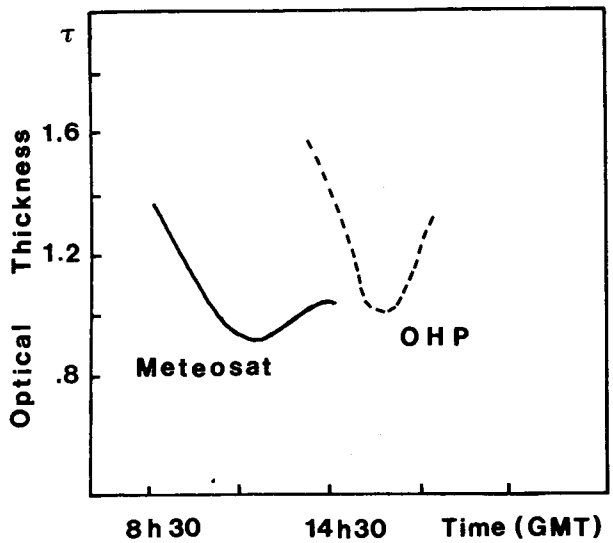

FIG. 7. Time evolution of the aerosol optical thickness derived from METEOSAT data at point P (solid line), and measured at the OHP (dashed line), on 27 July. The curve "METEOSAT" was roughly interpolated from the values of τ_a at P, at 0830, 1130 and 1430 UTC, derived from the maps in Fig. 5. The curve "OHP" was interpolated from the τ_a measurements (Fig. 1) performed at the OHP from 1330 to 1730 UTC. The two curves are consistent, taking into account the 6 h needed for the dust cloud to go from P to the OHP, a distance of about 120 km according to the observed wind speed of 20 km h^{-1}.

presence of large particles and is close to the value derived from the ground measurements. The $\tau_a(\lambda)$ measurements reported in Fig. 2 for 29 July at 648 and 864 nm (i.e., quite near from the AVHRR centroïd wavelengths) provide an Angström coefficient $\alpha_a = 0.66$ (close to the α_{IR} figure reported in Table 1). The good agreement between the two estimates indicates that α_a might be deduced from AVHRR data and could provide some information on the particle dimension evolution.

4. Conclusion

A dust cloud was observed with a photometric station from the ground, and, simultaneously, from two satellite imageries (METEOSAT and AVHRR). The optical thicknesses derived from the two experiments (ground and METEOSAT data) lead to good agreement. The Angström coefficient derived from the AVHRR data seems valid. It indicates a large mode of particles, also observed at the ground station. The METEOSAT B2 data allowed the dust outbreak to be seen and, also, the aerosol mass to be quantified by an estimation of the optical thickness. A climatology of Saharan dust using METEOSAT B2 data at climatic scales is now being developed.

Acknowledgments. This work was partly supported by the "Centre National de la Recherche Scientifique" (CNRS) and by the "Centre National d'Etudes Spatiales" (CNES).

REFERENCES

Carlson, T. N., and J. M. Prospero, 1972: The large scale movements of Saharan air outbreaks over the equatorial North Atlantic. *J. Appl. Meteor.* **11,** 289–297.

——, and P. Wendling, 1977: Reflected radiance measured by NOAA 3 AVHRR as a function of optical depth for Saharan dust. *J. Appl. Meteor.*, **16,** 1368–1371.

Deschamps, P. Y., M. Herman and D. Tanré, 1983: Modeling of the atmospheric effects, and its application to the remote sensing of ocean color. *Appl. Opt.*, **22,** 3751–3758.

Fouquart, Y., B. Bonnel, M. Chaoui Roquai, R. Santer and A. Cerf, 1987: Observation of Saharan aerosols: results of ECLATS field experiment, Part I: Optical properties and aerosol size distributions. *J. Climate Appl. Meteor.*, **26,** 28–37.

Fraser, R. S., 1976: Satellite measurements of mass of Saharan dust in the atmosphere. *Appl. Opt.*, **15,** 2471–2479.

Griggs, M., 1979: Satellite observations of atmospheric aerosols during the EOMET Cruise. *J. Atmos. Sci.*, **36,** 695–698.

Herman, M., J. Y. Balois, L. Gonzalez, P. Lecomte, J. Lenoble, R. Santer and C. Verwaerde, 1986: Stratospheric aerosol observations from a balloon-borne polarimetric experiment. *Appl. Opt.*, **25,** 3573–3584.

King, M. D., D. M. Byrne, B. M. Herman and J. A. Reagan, 1978: Aerosol size distribution obtained by inversion of spectral optical depth measurements. *J. Atmos. Sci.*, **35,** 2153–2167.

Kneizys, F. Y., E. P. Shettle, W. O. Gallery, J. H. Chetwind, Jr., L. W. Abren, J. E. A. Selby, R. W. Fenn and R. A. Mc Clatchey, 1980: Atmospheric transmittance/radiance: Computer code LOWTRAN 5, Rep. AFGL-TR-80-0067, 233 pp.

Koepke, P., 1982: Calibration of the vis-channel of Meteosat-2. *Adv. Space Res.*, **2,** 93–96.

——, and H. Quenzel, 1979: Turbidity of the atmosphere determined from satellite: Calculation of optimum viewing geometry. *J. Geophys. Res.*, **84,** 7847–7856.

Legrand, M., J. J. Bertrand and M. Desbois, 1985: Dust clouds over West Africa: A characterization by satellite data. *Ann. Geophys.*, **3,** 777–784.

London, J., R. D. Bojkov, S. Oltmans and J. I. Kelley, 1976: *Atlas of the Global Distribution of Total Ozone July 1957–June 1967.* NCAR Tech. Note, NCAR/TN/113+STR, pp 276.

Mc Clatchey, R. A., R. W. Fenn, J. E. A. Selby, F. E. Volz and J. S. Garing, 1971: Optical properties of the atmosphere. Rep. AFCRL-71-0279, pp 85.

Malika, W. A., and D. M. Anderson, 1986: Satellite data availability and calibration documentation for land surface climatology studies. Contract NAS5-28715, NASA, Goddard Space Flight Center, pp 214.

Mekler, Y., H. Quenzel, G. Ohring and J. Marcus, 1977: Relative atmospheric aerosol content from ERTS observations. *J. Geophys. Res.*, **82,** 967–970.

Norton, C. C., F. R. Mosher, B. Hinton, D. W. Martin, D. Santek and W. Kuklow, 1980: A model for calculating desert aerosol turbidity over the oceans from geostationary satellite data. *J. Appl. Meteor.*, **19,** 633–644.

Otterman, J., R. S. Fraser and O. P. Bahethi, 1982: Characterization of tropospheric desert aerosols at solar wavelengths by multispectral radiometry from Landsat. *J. Geophys. Res.*, **82,** 1270–1278.

Patterson, E. M., D. A. Gillette and B. M. Stockton, 1977: Complex index of refraction between 300 and 700 nm for Saharan aerosols. *J. Geophys. Res.*, **82,** 3153–3160.

Santer, R., 1984; Caractérisation des aérosols à partir de la polarisation du rayonnement solaire diffusé. Application aux atmosphères de la Terre, de Vénus et de Saturne. Thèse de Doctorat es Sciences Physiques. Université des Sciences et Techniques de Lille.

Weinman, J. A., J. T. Twitty, J. R. Browning and B. M. Herman, 1975: Derivation of phase functions from multiply scattered sunlight transmitted through a hazy atmospheric. *J. Atmos. Sci.*, **32,** 577–583.

World Meteorological Organization, 1986: A preliminary cloudless standard atmosphere for radiation computation. WCP-112, WMO/TD-n°24, pp 53.